

ADVANCED ENERGY MATERIALS

Supporting Information

for *Adv. Energy Mater.*, DOI: 10.1002/aenm.201900940

Boosting the Performance of WO₃/n-Si Heterostructures for Photoelectrochemical Water Splitting: from the Role of Si to Interface Engineering

*Yihui Zhao, Geert Brocks, Han Genuit, Reinoud Lavrijsen, Marcel A. Verheijen, and Anja Bieberle-Hütter**

Supporting Information

Boosting the Performance of WO₃/n-Si for Photo-electrochemical Water Splitting: the Role of Si to Interface Engineering

*Yihui Zhao, Geert Brocks, Han Genuit, Reinoud Lavrijsen, Marcel A Verheijen, Anja Bieberle-Hütter**

Films deposition

Table 1

Sputtering process parameters for WO₃ deposition.

Parameter	Value
Target power	100 W
Base pressure	<10 ⁻⁸ mbar
Deposition pressure	10 ⁻² mbar
Substrate temperature	Room temperature
O ₂ flow rate	10 sccm
Ar flow rate	40 sccm

Figure S1 shows the flow diagram of the thin film depositions.

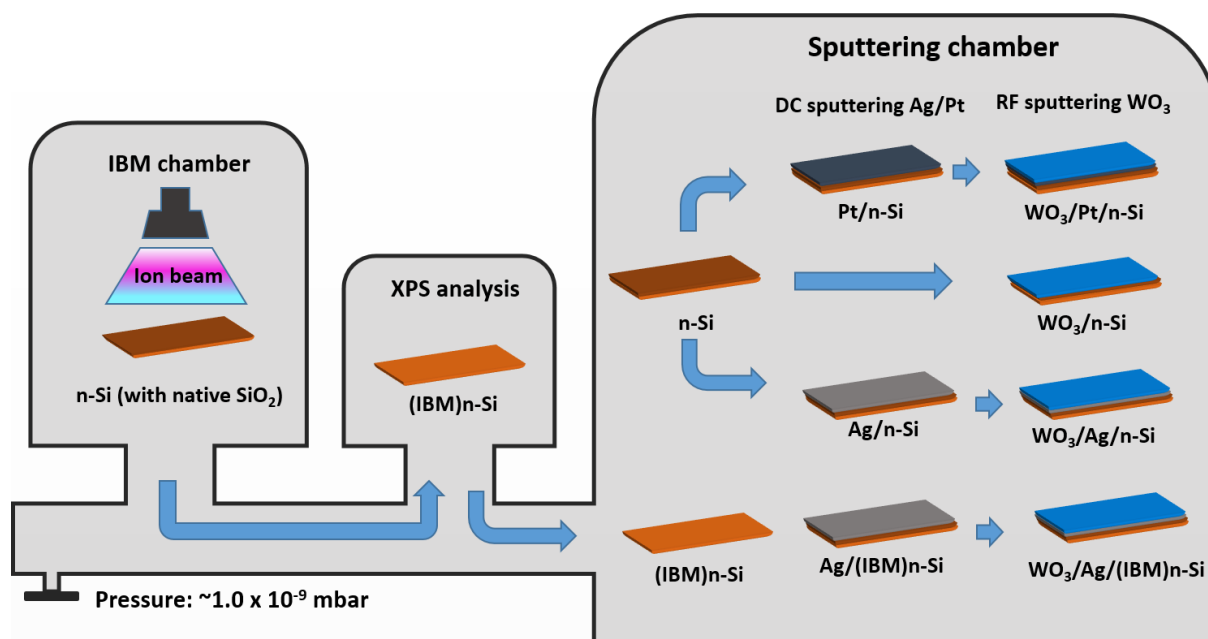


Figure S1: Flow diagram of WO₃/n-Si, WO₃/Ag/n-Si, WO₃/Ag/(IBM)n-Si (ion beam milling treated n-Si) and WO₃/Pt/n-Si deposition. The entire process is carried out without breaking the vacuum.

Atomic Force Microscope (AFM) of WO₃/n-Si and WO₃/FTO

Figure S2 shows the surface roughnesses of WO₃/n-Si and WO₃/FTO, which were measured by AFM. The surface roughnesses of WO₃/n-Si and WO₃/FTO are $R_a = 2.2$ nm and $R_a = 7.1$ nm, respectively.

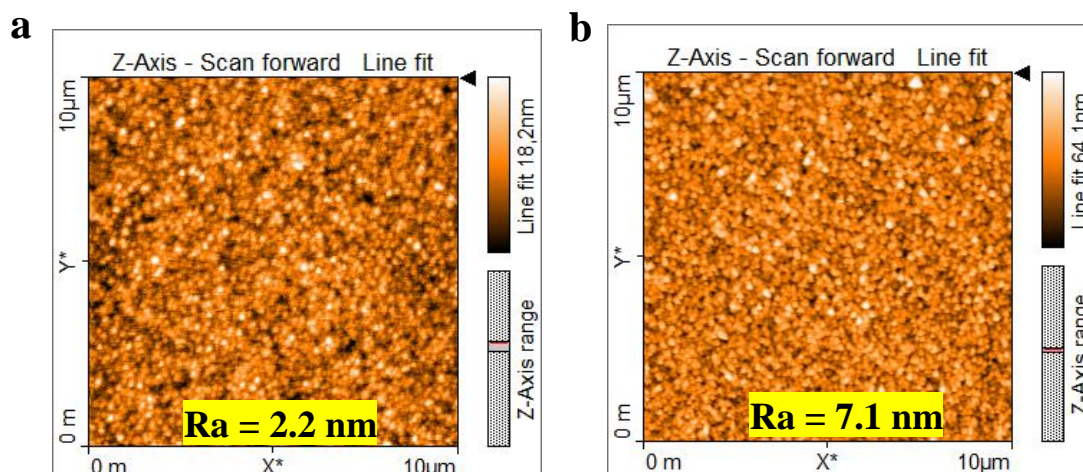


Figure S2: Atomic Force Microscope (AFM) of (a) WO₃/n-Si and (b) WO₃/FTO after annealing in the Ar.

Cross-section HAADF-STEM of WO₃/n-Si and WO₃/FTO

Cross-section HAADF-STEM images confirm that an intimate contact is obtained for both WO₃/n-Si and WO₃/FTO interfaces, as shown in Figure S3.

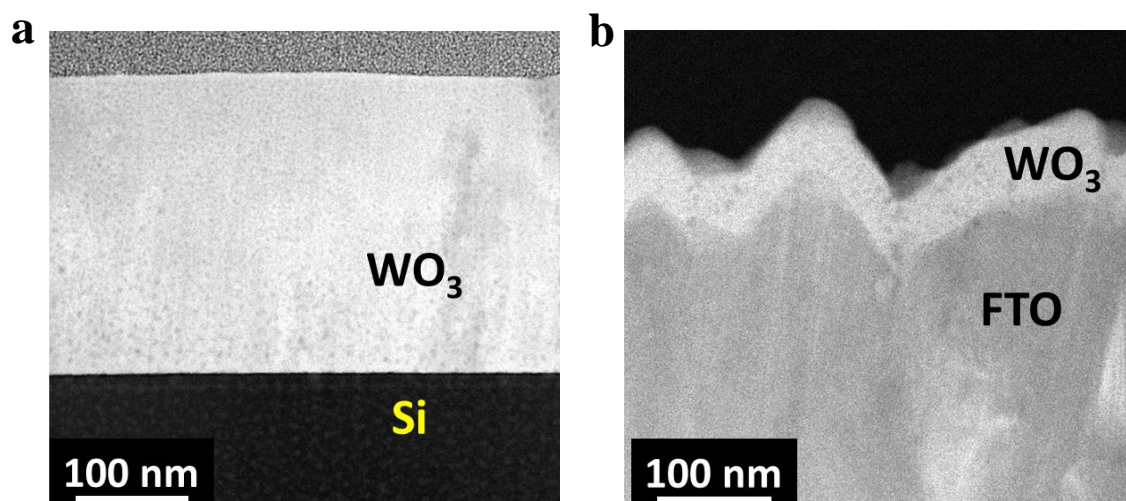


Figure S3: Cross-section HAADF-STEM images of (a) WO₃/n-Si and (b) WO₃/FTO.

GIXRD of WO₃/n-Si and WO₃/FTO

The GIXRD spectra of the WO₃/n-Si and WO₃/FTO after annealing in Ar at 450°C for 1 h are shown in Figure S4. The diffraction peaks agree well with monoclinic WO₃ corresponding to JCPDS No. 83-0950 indicating that monoclinic WO₃ was obtained for both electrodes after annealing.

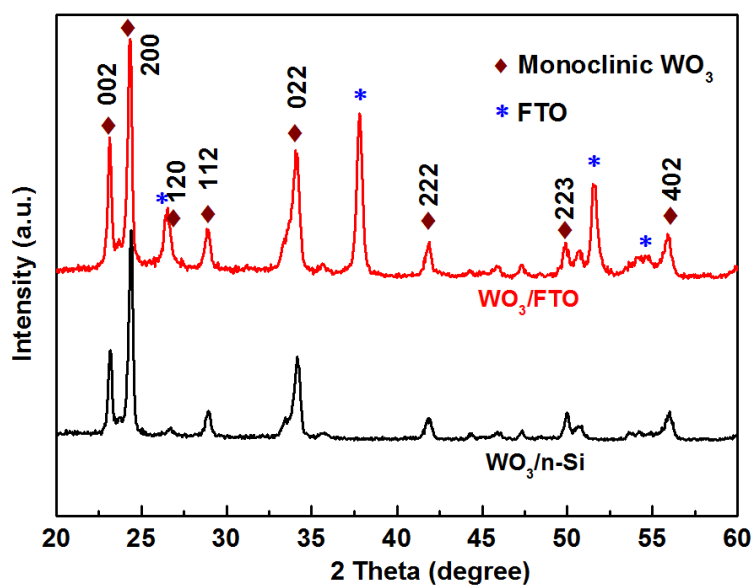


Figure S4: GIXRD spectra of $\text{WO}_3/\text{n-Si}$ (black) and WO_3/FTO (red) after annealing in Ar. The brown diamonds and the blue dots are monoclinic WO_3 (JCPDS No. 83-0950) and FTO (JCPDS No. 83-0950), respectively.

Relative energy band levels

Figure S5 shows the energy band diagrams of n-Si, WO_3 , Ag, Pt and H_2O . The band gap of n-Si is $\sim 1.1 \text{ eV}^{[1]}$ and the Fermi level is about $-4.25 \pm 0.1 \text{ eV}$ vs vacuum level^[1-3]. The band gap of WO_3 is about 2.8 - 3.0 eV and the Fermi level is about $-5.25 \pm 0.1 \text{ eV}^{[4-7]}$. The work functions of Ag and Pt are $4.5 \pm 0.15 \text{ eV}$ and $5.7 \pm 0.1 \text{ eV}$ vs vacuum level^[8].

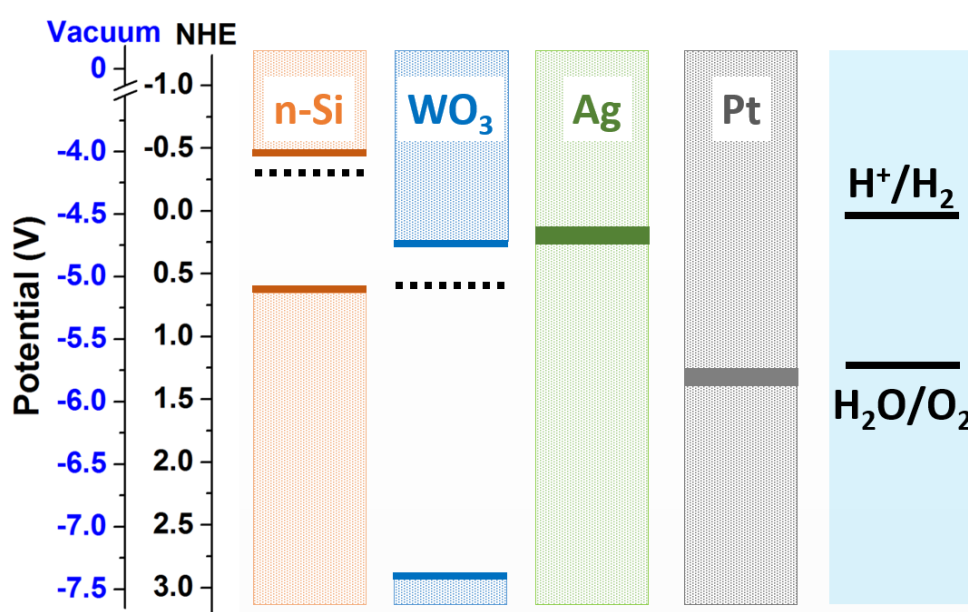


Figure S5: Diagram of relative energy band levels of n-Si, WO_3 , Ag, Pt, and H_2O . The diagram is constructed from literature data^[1-8].

Reference

- [1] S. Y. Reece, J. a. Hamel, K. Sung, T. D. Jarvi, a. J. Esswein, J. J. H. Pijpers, D. G. Nocera, *Science* **2011**, 334, 645.
- [2] M. T. Mayer, C. Du, D. Wang, *J. Am. Chem. Soc.* **2012**, 134, 12406.
- [3] Y. J. Hwang, A. Boukai, P. Yang, *Nano Lett.* **2009**, 9, 410.
- [4] Y. Zhao, S. Balasubramanyam, R. Sinha, R. Lavrijsen, M. A. Verheijen, A. A. Bol, A. Bieberle-Hütter, *ACS Appl. Energy Mater.* **2018**, 1, 5887.
- [5] P. Dias, T. Lopes, L. Meda, L. Andrade, A. Mendes, *Phys. Chem. Chem. Phys.* **2016**, 5232.

- [6] H. Li, H. Yu, X. Quan, S. Chen, Y. Zhang, *ACS Appl. Mater. Interfaces* **2016**, 8, 2111.
- [7] J. Y. Zheng, A. U. Pawar, C. W. Kim, Y. J. Kim, Y. S. Kang, *Appl. Catal. B Environ.* **2018**, 233, 88.
- [8] J. Hölzl, F. K. Schulte, H. Wagner, *Solid Surface Physics*; Springer-Verlag Berlin, 1979.